Temperature-Gradient-Driven Tearing Modes

A. Botrugno 1), P. Buratti 1), B. Coppi 2)

1) EURATOM-ENEA Fusion Association, Frascati (RM), Italy
2) Massachussets Institute of Technology, Cambridge (MA), USA

e-mail contact of main author: antonio.botrugno@frascati.enea.it

Abstract. The observation of spontaneous islands growth in tokamak experiments indicates that the tearing mode could also be linearly unstable. However, in the framework of resistive magnetohydrodynamics, previous works have demonstrated that drift effects, electron heat transport along magnetic field lines and ion Larmor radius effects have stabilizing effects. Recently, numerical calculations and analytical theory in the collisional regime have demonstrated that inclusion of perpendicular electron heat transport carries out a new type of linear tearing mode driven by a large electron temperature gradient. In this paper, we review the linear tearing mode equations in order to identify the relevant instability regimes. The relevance of some regimes to experiments is discussed and analytical results in different regimes are presented. In all cases, realistic value of the perpendicular electron heat transport produces a strong destabilizing term proportional to the electron temperature gradient in the expression of the island growth rate.

1. Introduction

Tearing instabilities are related to a deformation of the magnetic field topology leading to generation of magnetic islands via magnetic reconnection due to finite plasma resistivity. The presence of magnetic islands degrades confinement and is presently a major limit to the achievement of high beta plasmas. The physical mechanism of tearing modes onset remains an outstanding problem of magnetic confinement.

In the simplest model of linear resistive magnetohydrodynamics, the stability of tearing modes is ruled by the Δ' parameter, which represents the convexity of the mode eigenfunction at the resonant surface $(\mathbf{k}\cdot\mathbf{B}=0)$. If $\Delta'>0$ current filamentation is energetically favourable and the mode is unstable. Modes with poloidal number $m>2$ typically have $\Delta'<0$. Drift-tearing theories involving the combined effect of magnetic reconnection, electron density and temperature gradients resulted in slower growth rate and instability condition $\Delta'>\Delta'_{crit}$, Δ'_{crit} being a large positive threshold [1-3]. All these theories included parallel electron energy transport as a key ingredient but neglected the perpendicular one. These results were in marked contrast with experiments, in which tearing modes are often observed. In order to resolve this contrast tearing modes were assumed to be metastable, i.e. growing from a seed island generated by other instabilities such as sawtooth crashes, fishbones or edge localized modes (ELMs). However, tearing modes can also grow without any trigger event. Spontaneous tearing modes have been observed in JET hybrid discharges [4] in FTU discharges and in various TFTR discharges [5]. These observations indicate that tearing mode could be linearly instable.

More recently, analytic theory in the collisional regime [6] and numerical modelling in collisional and weakly collisional regimes [7, 8] have demonstrated that, with the inclusion of realistic values of the (anomalous) perpendicular electron heat diffusivity, a new type of linear tearing mode appears, which is driven unstable even at $\Delta'<0$ by a sufficiently large electron temperature gradient.

In this paper the results of linear analytical theory are reviewed and extended to a weakly collisional regime. The paper is organized as follows. In section 2 the experimental background is presented and realistic values of the key parameters are determined. In section 3 the basic equations are presented and different instability regimes are highlighted. In section 4 results relevant to the different regimes are summarized. Concluding remarks are given in section 5.

2. Experimental background

Tearing modes can grow without any trigger event in tokamak experiments. This has been clearly observed in various discharges in the hybrid regime of JET, with high normalized kinetic pressure (β_N). It is usually difficult to distinguish tearing modes which grow spontaneously from metastable tearing modes, because of the MHD activity normally present in the hybrid regime as fishbones, internal kink modes, Alfven eingemode, and especially ELMs can disturb the interpretation of experimental signals. However, in some cases, there are no doubts about the spontaneous growth of tearing modes. As example, we show in FIG. 1 (lower frame) the spectrogram of a magnetic coils signal in JET discharge 57826. Two tearing modes with toroidal number n=3 and n=2 grow in absence of any other MHD instabilities, the first one after 5.3 s. with frequencies between 20 and 25 kHz, the second one after 5.6 s. at about 15 kHz.

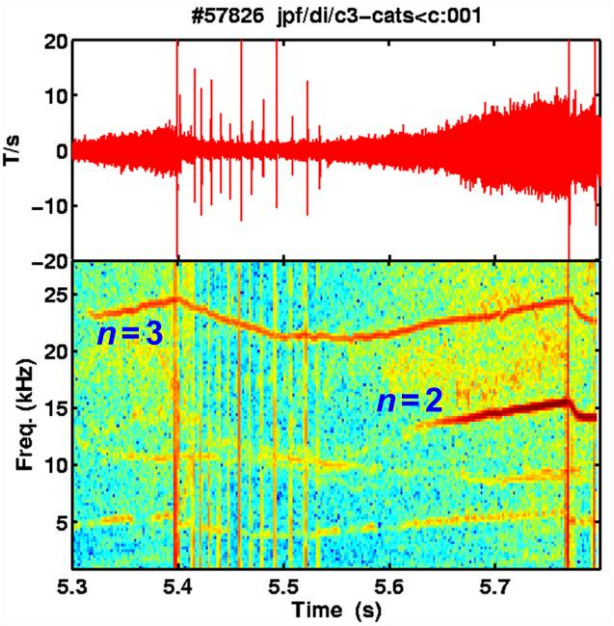

FIG. 1. Magnetic coil signal (upper frame) and its spectrogram (lower frame) in JET discharge number 57826. Spikes in the signal are due to ELMs. Tearing modes with toroidal numbers n=2 and 3 can be seen as continuous red lines in the spectrogram. Both modes appear during ELM-free periods.

Similar phenomenology can be observed in FTU discharges. As example, we show in FIG. 2 (upper frame) the spectrogram of a magnetic coil signal in the discharge number 25568. It is evident a tearing mode with toroidal and poloidal number n=1 m=2 at 6 kHz starting at about 0.68 s. without any other evident MHD activities.

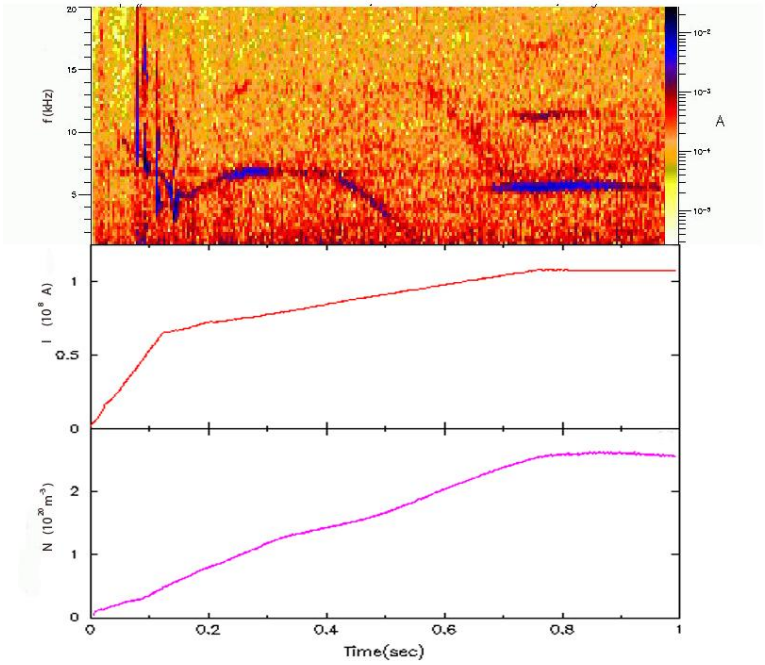

FIG. 2. Spectrogram of magnetic coil signal (upper frame), current (central frame) and density (lower frame) in FTU discharge number 25568. Tearing modes with toroidal number n=1 can be seen as continuous dark lines in the spectrogram.

TABLE I: CHARACTERISTIC FREQUENCIES AND LENGTHS FOR DISCUSSED DISCHARGES

	$\omega^*/2\pi$ (kHz)	ν_{ei} (kHz)	ρ_S (mm)	Δ_D (mm)	Δ_c (mm)	$\Delta_\perp$ (mm)	d_e (mm)
JET	6	50	6.0	2	3	3	0.8
FTU	0.5	1300	0.4	3	1.1	4.5	0.4

Values are calculated from experimental data, assuming perpendicular heat diffusivity values of 1 m^2/s, classical parallel heat conduction and Spitzer resistivity. JET Data are evaluated at onset of the n=2 mode shown in FIG. 1. FTU data are evaluated at mode shown in FIG. 2 and t=0.7 s.

3. Basic equations of the linear model

We describe the tearing mode as a perturbation with frequency ω and wave vector **k** directed along y, in a sheared slab with shearing length L_S in x direction. The electromagnetic fields are given by

$$\mathbf{E} = -\frac{1}{c}\frac{\partial A}{\partial t}\hat{\boldsymbol{z}} - \nabla\boldsymbol{\phi} \qquad \text{and} \qquad \mathbf{B} = B\hat{\boldsymbol{z}} - \nabla A \times \hat{\boldsymbol{z}}$$

where A is the z-component of the vector electromagnetic potential and $\boldsymbol{\phi}$ is the scalar electromagnetic potential.

We consider a set of Braginskii-type transport equations in two fluids form. We assume linear expansions of the form $F = f_0(x) + f(x)\exp(iky - i\omega t)$, and notation with 0 subscript for equilibrium quantities and without subscript for perturbations.

The first equation of the linear system is the parallel electron momentum balance equation, in which pressure gradient and thermal force effects are included:

$$\eta \mathbf{B}\cdot\mathbf{j} = \mathbf{B}\cdot\mathbf{E} + \frac{1}{en}\mathbf{B}\cdot\nabla p + \frac{\alpha}{e}\mathbf{B}\cdot\nabla T \qquad (1)$$

Where *n*, *p* and *T* are electron density, pressure and temperature, *e* is the unit charge and α=0.71 is the thermal force coefficient.

The parallel gradient operator to first order of linear expansion becomes $\frac{\mathbf{B}\cdot\nabla}{B} = k_{\parallel} + \frac{B_x}{B_0}\frac{\mathrm{d}}{\mathrm{d}x}$, where $k_{\parallel} = \frac{\mathbf{B}\cdot\mathbf{k}}{B} \approx \frac{kx}{L_S} \equiv k_{\parallel}' x$ and $B_x = ikA$. The total time derivative is $\frac{\mathrm{d}}{\mathrm{d}t} = -i\omega - i\frac{ck\phi}{B_0}\frac{\mathrm{d}}{\mathrm{d}x}$. The x-derivatives give rise to diamagnetic frequencies of the form $\omega_{*f} = -\frac{kcT_0}{eB_0 f_0}\frac{\mathrm{d}f_0}{\mathrm{d}x}$. The parallel electric field is $E_{\parallel} = i\frac{\omega}{c}A - ik_{\parallel}\phi$. Then, equation (1) can be rewritten as

$$\eta j_{\parallel} = i\frac{\omega}{c}A - ik_{\parallel}\phi + \frac{T_0}{en_0}ik_{\parallel}n - i\frac{\omega_{*n}}{c}A + \frac{1+\alpha}{e}ik_{\parallel}T - i\frac{(1+\alpha)\omega_{*T}}{c}A$$

or, defining $\delta\omega = \omega - \omega_{*n} - \hat{\alpha}\omega_{*T}$ and $\hat{\alpha} = 1 + \alpha = 1.71$, as

$$\eta j_{\parallel} = i\frac{\delta\omega}{c}A - ik_{\parallel}\phi + ik_{\parallel}\frac{T_0}{en_0}n + ik_{\parallel}\frac{\hat{\alpha}}{e}T \qquad (2)$$

The second equation is the parallel electron continuity equation which has the form

$$\frac{dn}{dt} = D_{\perp}\frac{\partial^2 n}{\partial^2 x} + + \frac{1}{e}(\nabla j)_{\parallel} \qquad (3)$$

Neglecting perpendicular particle diffusion $D_{\perp} = 0$, the previous equation can be written as

$$\omega n = \omega_{*n} n_0 \frac{e\phi}{T_0} - \frac{1}{e}k_{\parallel}j_{\parallel} \qquad (4)$$

and using equation (2) to eliminate $j_{\parallel}$ we obtain

$$(x^2 - i\Delta_D^2)n = -x\frac{en_0}{k_{\parallel}'T_0}\frac{\delta\omega}{c}A - x^2\frac{\hat{\alpha}n_0}{T_0}T + \frac{en_0}{T_0}\left(x^2 + i\frac{\omega_{*n}}{\omega}\Delta_D^2\right)\phi \qquad (5)$$

with $\Delta_D = \left(\frac{\omega}{k_{\parallel}'^2}\frac{\eta e^2 n_0}{T_0}\right)^{1/2} = \frac{\sqrt{\omega\nu_{ei}}}{k_{\parallel}'v_e}$, where ν_{ei} and v_e are collision frequency an electron thermal velocity respectively. The Δ_D parameter gives the length scale of density response; values calculated for the experimental examples are given in Table I.

The third equation is the parallel charge neutrality equation in the limit of strongly magnetized ions

$$k_{\parallel}j_{\parallel} = -\frac{c^2(\omega-\omega_{di})}{4\pi V_A^2}\frac{\mathrm{d}^2\phi}{\mathrm{d}x^2} \qquad (6)$$

where V_A is the Alfvén velocity and ω_{di} is the ion diamagnetic frequency. Substituting $j_{\parallel}$ from (2) and *n* from (3) we have

$$\left(\rho_s^2 - i\frac{\Delta_C^4}{x^2}\right)\frac{\mathrm{d}^2\phi}{\mathrm{d}x^2} = \left(1 \pm \frac{\omega_{*n}}{\omega}\right)\phi - \frac{\delta\omega}{ck_\parallel' x}A - \frac{\hat{\alpha}}{e}T$$

where $\rho_s^2 = T_0/m_i\Omega_{\mathrm{ci}}^2$ is the ion sound Larmor radius and $\Delta_C^4 = \frac{\eta c^2(\omega-\omega_{di})}{4\pi V_A^2 k_\parallel'^2} \approx \rho_s^2\Delta_D^2$. The spatial scale for the electrostatic potential is then Δ_C if $\Delta_C \gg \rho_s$ and ρ_s if $\rho_s \gg \Delta_C$. Equation (6) only holds if the ion larmor radius is smaller than the current layer width, otherwise a form accounting for non-local effects has to be used [3].

The fourth equation is the electron energy balance equation

$$\frac{3}{2}(-i\omega T + i\omega_{*T}e\phi) = \chi_\perp\frac{\mathrm{d}^2T}{\mathrm{d}x^2} - k_\parallel^2\chi_\parallel \mathrm{T} + k_\parallel\chi_\parallel\omega_{*T}\frac{e}{c}A + i\frac{\hat{\alpha}}{e}\frac{T_0}{n_0}k_\parallel j_\parallel \qquad (7)$$

where $\chi_\perp$ and $\chi_\parallel$ are perpendicular and parallel electron heat diffusivities. Introducing the characteristic lengths $\Delta_\perp = \left(\frac{\chi_\perp}{k_\parallel'^2\chi_\parallel}\right)^{1/4}$ and $\Delta_\parallel = \left(\frac{3}{2}\frac{\omega}{k_\parallel'^2\chi_\parallel}\right)^{1/2}$, equation (7) can be recast as

$$\Delta_\perp^4\frac{\mathrm{d}^2T}{\mathrm{d}x^2} - x^2\mathrm{T} + \frac{x\omega_{*T}}{k_\parallel'}\frac{e}{c}A - i\frac{\omega_{*T}}{\omega}\Delta_\parallel^2 e\phi + i\Delta_\parallel^2\mathrm{T} + \frac{2}{3}i\frac{\hat{\alpha}}{e}\frac{T_0}{n_0}\frac{k_\parallel' x}{\omega}\Delta_\parallel^2 j_\parallel = 0 \qquad (8)$$

For classical $\chi_\parallel$ and η we have $\frac{2}{3}\chi_\parallel = 1.07\frac{T_0}{\eta e^2 n_0}$ and the parallel transport scale $\Delta_\parallel = 0.97\Delta_D$. Moreover we have the Ampère law and the boundary condition

$$-\frac{4\pi}{Ac}\int_{-\infty}^{\infty} j_\parallel dx = \frac{1}{A}\int_{-\infty}^{\infty} A"dx = \Delta' \qquad (9)$$

Where $\boldsymbol{\Delta'}$ is the jump in the logarithmic derivate of B_x inside the slab

$$\Delta' \equiv \left|\frac{d}{dx} ln\, A\right|_{x=-0}^{x=+0}$$

We express the dispersion relation of the perturbation in the form $\omega = \omega_R + i\gamma$, it can be obtained by solving equations (2) and (4) for $j_\parallel$ and integrating the result according to (9). In the following we assume the "constant *A* approximation", which can be applied if magnetic diffusion across the current layer during one oscillation cycle is negligible. Analytical solutions in different regimes will be considered in the following. Different regimes of collisionality depend on the ordering of the characteristic lengths:

- ***Collisional regime*** $\boldsymbol{\Delta_D \gg \rho_s}$. In this case $\Delta_D \gg \Delta_C$, so that the spatial variation of potential is more rapid than that of density and temperature. The inductive term $\frac{\delta\omega}{c}A$ in equation (2) is then balanced by the electrostatic one $k_\parallel\phi$ and the spatial width of $j_\parallel$ is Δ_C. This regime clearly applies to FTU data in Table I.

- ***Semicollisional regime*** $\boldsymbol{\Delta_D \ll \rho_s}$. In this case $\Delta_D \ll \Delta_C$, so the inductive term is compensated by density and temperature perturbations and the spatial width of $j_\parallel$ is Δ_D. This regime applies for JET data as given in Table I, but it is important to notice that interaction between microturbulence and the tearing mode can increase the

effective electron collision frequency and restore the collisional regime even at high plasma temperature [6], (see also section 4.2).

- ***Collisionless regime***. The electron motion becomes insensitive to collisions if the electron mean free path λ_{mfp} is larger than the parallel wavelength, i.e. if $k_\parallel \lambda_{mfp} \gg 1$. Using $k_\parallel \approx k_\parallel^{'} \Delta_D$, the condition reduces to $\omega \gg \nu_{ei}$.

4. Analytical results

4.1. Negligible perpendicular transport $\boldsymbol{\Delta_\perp = 0}$

This case was treated in references [2, 3] for different collisionality regimes. The general finding was that the temperature gradient plays a stabilizing role. This is particularly simple to illustrate in the semicollisional regime, for which $\omega_R \approx \omega_{*n} + 0.5\hat{\alpha}\omega_{*T}$ and $\gamma \approx \frac{c^2\eta}{4\pi}\frac{\Delta^{'}}{\Delta_D} - \frac{\pi^2}{2}\frac{(\omega_R-\omega_{*n})^{3/2}}{\sqrt{\omega}}\frac{\Delta_D}{\rho_s}$. The second term in γ is stabilizing and it is proportional to $(\omega_{*T})^{3/2}$.

4.2 Collisional case with strong perpendicular transport $\boldsymbol{\rho_s \ll \Delta_C \ll \Delta_\perp}$

This case was treated in reference [1]. The dispersion relation yields $\omega_R = \omega_{*n} + \hat{\alpha}\omega_{*T}$ and $\gamma = a_1\frac{c^2\eta}{4\pi}\frac{\Delta^{'}}{\Delta_C} + a_2\omega_R\left(\frac{\Delta_C}{\Delta_\perp}\right)^3$, where a_1, a_2 are numerical coefficient of order one. The growth rate can be positive even with negative values of the $\Delta^{'}$ index, i.e. as a consequence of perpendicular heat transport the temperature gradient can drive the instability even if the current profile is stabilizing. In the same paper the possibility of collisionality enhancement by microscopic reconnecting modes was proposed. The enhancement factor is $1 + \frac{\omega_*}{\nu_{ei} k d_e}$; with this, the condition $\Delta_C > \rho_s$ would apply in all experimental conditions.

4.3. Semicollisional case with strong perpendicular transport $\boldsymbol{\Delta_D \ll \Delta_\perp \ll \rho_s}$

In this case the electric potential varies on the largest length scale, so that it remains negligible across the current channel width. Use of equation 6 in this regime requires $\rho_i \ll \rho_S$, which does not apply to experiments like JET, in which $T_i \geq T_e$. Nevertheless, this ordering allows the most transparent derivation of the dispersion relation, so it is instructive to consider it. Equation (2) becomes

$$-i\eta j_\parallel = \frac{\Delta_D^2}{\Delta_D^2 + ix^2}\frac{\delta\omega}{c}A + \frac{k_\parallel^{'}x}{e}\hat{\alpha}T\frac{\Delta_D^4 + ix^2\Delta_D^2}{\Delta_D^4 + x^4} \qquad (10)$$

Temperature can be calculated explicitly since $\Delta_\parallel \approx \Delta_D \ll \Delta_\perp$, so that the energy balance equation reduces to

$$\Delta_\perp^4 \frac{\mathrm{d}^2T}{\mathrm{d}x^2} - x^2\mathrm{T} + \frac{x\omega_{*T}}{k_\parallel^{'}}\frac{e}{c}A = 0, \qquad (11)$$

In the following we use the constant A approximation, which requires $\frac{4\pi\Delta_D^2\omega}{c^2\eta} \ll 1$. In this approximation the solution of equation (11) is

$$T(x) = \frac{\omega_{*T}}{k_\parallel' \Delta_\perp} \frac{e}{c} A \frac{z}{2} \int_0^{\pi/2} d\theta \sqrt{\sin\theta} \exp\left[-\frac{z^2 \cos\theta}{2}\right]$$

with $z = x/\Delta_\perp$. The dispersion relation gives $\omega_R = \omega_{*n} + \hat{\alpha}\omega_{*T}$ and

$$\gamma = \frac{c^2 \eta}{4\pi} \frac{\Delta'}{\sqrt{2\pi}|\Delta_D|} + \frac{\hat{\alpha}|\omega_{*T}|}{\sqrt{2\pi}} \left|\frac{\Delta_D}{\Delta_\perp}\right| \left(\mathrm{I_i} - \left|\frac{\Delta_D^2}{\Delta_\perp^2}\right| \mathrm{I_r}\right)$$

where $\left|\frac{\Delta_D^2}{\Delta_\perp^2}\right| \mathrm{I_r} = \left|\frac{\Delta_D^2}{\Delta_\perp^2}\right| \int \frac{zY(z)}{z^4 + \Delta_D^4/\Delta_\perp^4} \mathrm{d}z \cong 0$ and $\mathrm{I_i} = \int \frac{z^3 Y(z)}{z^4 + \Delta_D^4/\Delta_\perp^4} \mathrm{d}z = 2.78$

with $Y(z) = \frac{z}{2} \int_0^{\pi/2} d\theta \sqrt{\sin\theta} \exp\left[-\frac{z^2 \cos\theta}{2}\right]$.

In the $\Delta_\perp = 0$ case the scale of temperature variation is Δ_D instead of $\Delta_\perp$ (see FIG. 3) and the *T*-term in (10) gives no contribution to the growth rate. The key effect of $\chi_\perp$ is to increase the distance between the resonant surface ($\mathbf{k}\cdot\mathbf{B} = 0$) and the isothermal region, in which $\mathbf{B}\cdot\nabla T = 0$. For $\chi_\perp = 0$ the distance is $\Delta_D = \left(\omega/\chi_\parallel\right)^{1/2} L_S/k$ [2]; the corresponding temperature perturbation is shown by the blue curve in figure 1. With realistic values of $\chi_\perp$, the profile is smoother (red trace in figure 1) and the isothermal region is shifted to $\Delta_\perp \gg \Delta_\parallel$.

The negative contribution $\approx \Delta_D/\rho_s$ found in [2] for the semicollisional regime (see section 4.1) does not appear in the growth rate expression since terms of first order in Δ_D/ρ_s have been neglected in equations (10) and (11).

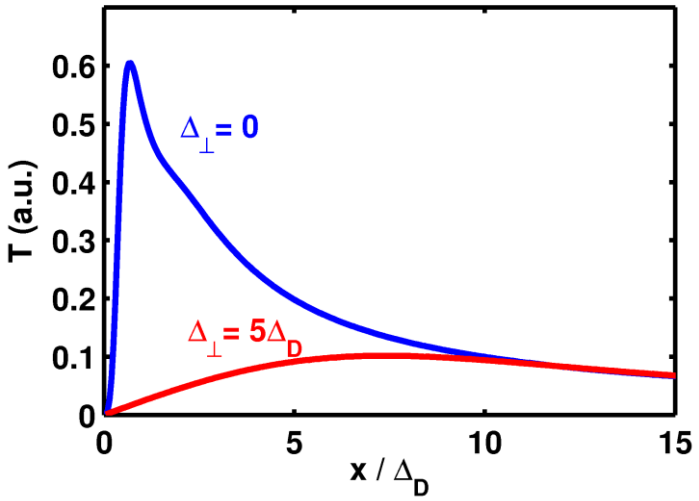

FIG. 3. Profiles of the electron temperature eigenfunctions with negligible (blue) and realistic (red) perpendicular transport versus normalized distance from the resonant surface.

5. Discussion

The possibility of tearing modes driven by the temperature gradient has been demonstrated in different asymptotic regimes (see sections 4.2 and 4.3). Similar results were obtained by including perpendicular heat transport in numerical simulations [7, 8]. These results point to a new interpretation of observations on spontaneous tearing modes. Comparison between

analytic results and JET data is not possible because separation of length scales is not large enough, while results from section 4.2 can be applied to the collisional (FTU) experimental case. With the parameters given in Table I, the mode turns out unstable unless $\Delta'/k = -14$ (the typical result of Δ' calculations being $\Delta'/k = -1$). This shows that the temperature gradient drive is a strong effect, and raises the question about what prevents tearing modes growth becoming ubiquitous).

References

[1] B. COPPI et al., Phys. Rev. Lett. **42** (1979) 1058
[2] J.F. DRAKE et al., Phys. Fluids **26** (1983) 2509
[3] S.C. COWLEY, R.M. KULSRUD AND T.S. HAHM, Phys. Fluids **29** (1986) 3230
[4] P. BURATTI et al., 34th EPS Conf. on Plasma Phys, Warsaw, July 2-6 2007 ECA **31F** O4018
[5] E.D. FREDRICKSON, Phys. Plasmas **9** (2002) 548
[6] B. COPPI, in "Collective phenomena in macroscopic systems" Eds. G.Bertin, Publ. Word Scientific, 2007
[7] Q. YU, S. GÜNTER, B.D. Scott, Phys. Plasmas **10** (2003) 797
[8] S. NISHIMURA ET AL., J. Phys. Soc. Jpn **76** (2007) 064501